Otology & Neurotology
32:1500–1505 © 2011, Otology & Neurotology, Inc.

Accuracy of Computed Tomography Detection of Superior Canal Dehiscence

*Sunitha M. Sequeira, †Bruce R. Whiting, †Joshua S. Shimony, †Katie D. Vo, and *‡Timothy E. Hullar

**Otolaryngology–Head and Neck Surgery, †Mallinckrodt Institute of Radiology, and ‡Anatomy and Neurobiology, Washington University School of Medicine, St. Louis, Missouri, U.S.A.*

Hypothesis: High-resolution temporal bone computed tomography (CT) may erroneously demonstrate a superior semicircular canal dehiscence (SSCD) where none exists and inaccurately display the size of a dehiscence.
Background: CT is an integral component of the diagnosis of SSCD. The prevalence of dehiscence as measured on computed tomographic scan is approximately eightfold higher than that on histologic studies, suggesting that CT may have a relatively low specificity for identifying canal dehiscence. This, in turn, can lead to an inappropriate diagnosis and treatment plan.
Methods: We quantified the accuracy of CT in identifying a dehiscence of the superior semicircular canal in a cadaver model using microCT as a gold standard. The superior canals of 11 cadaver heads were blue lined. Twelve of the 22 ears were further drilled to create fenestrations of varying sizes. Heads were imaged using medical CT, followed by microCT scans of the temporal bones at 18-μm resolution. Diagnosis of dehiscence and measurements of dehiscence size were performed on clinical CT and compared with that of microCT.
Results: Clinical CT identified 7 of 8 intact canals as dehiscent and tended to overestimate the size of smaller fenestrations, particularly those surrounded by thin bone.
Conclusion: These findings confirm that medical CT cannot be used as the exclusive gold standard for SSCD and that, particularly for small dehiscences on CT, clinical symptoms must be clearly indicative of a dehiscence before surgical treatment is undertaken. Preoperative counseling for small dehiscences may need to include the possibility that no dehiscence may be found despite radiologic evidence for it. **Key Words:** Computed tomography—Superior semicircular canal dehiscence syndrome—Vestibular—Third mobile window—Vertigo—Diagnosis.
Otol Neurotol **32:**1500–1505, 2011.

Superior semicircular canal dehiscence (SSCD) syndrome is diagnosed by a set of characteristic symptoms, pressure-induced vertical-torsional nystagmus, high-resolution temporal bone computed tomography (CT), and ancillary audiologic testing (1–4). The standard radiologic evaluation of patients suspected of having SSCD is a fine-cut (0.5- to 0.6-mm collimation) multi-slice temporal bone CT with reformatting of images parallel (Pöschl's view) and orthogonal (Stenver's view) to the plane of the superior semicircular canal (3). Accuracy of CT is paramount because the finding of SSCD on CT in a patient with debilitating symptoms may lead to a craniotomy or other surgical approach for repair. However, some evidence suggests that current CT imaging overestimates the prevalence of SSCD. Among 1,000 temporal bones evaluated histologically, the prevalence was 0.5% (5); in contrast, in a group of 581 temporal bone computed tomographic scans performed for a range of indications, the prevalence was 4% (6).

Inaccuracies in clinical computed tomographic scanning of superior canal dehiscence have been attributed to partial volume averaging (3,7). The finest image resolution reported in the literature is 100-μm pixel size after image reconstruction, with 100- to 500-μm increments (3,6,8). MicroCT scanning is able to achieve much better resolution than conventional clinical computed tomographic scanning, reducing or eliminating the chance for error, but cannot be performed on patients because of high radiation dosage, long scanning time, and size limitations. In this study, we performed microCT scanning of canal dehiscences in a cadaveric model, comparing the results with those obtained using conventional computed tomographic scanning. We hypothesized that, using microCT as a gold standard, we would find that clinical computed tomographic scans may inaccurately identify a dehiscence where none exists or overestimate the size of a dehiscence that is actually present.

Address correspondence and reprint requests to Timothy E. Hullar, M.D., Department of Otolaryngology–Head and Neck Surgery, Washington University School of Medicine, Campus Box 8115, 660 South Euclid Avenue, St. Louis, MO 63110; E-mail: hullart@ent.wustl.edu

Supported by American Academy of Otolaryngology–Head and Neck Surgery Foundation Resident Research Grant 175033 (S. M. S.) and National Institutes of Health K08 DC006869 (T. E. H.).

The authors report no conflicts of interest.

MATERIALS AND METHODS

Eleven fresh cadaver heads were used to create an anatomic model for superior canal dehiscence. Heads had been frozen and thawed once and stored in appropriate refrigeration thereafter, without fixation. Canal dehiscences of varying sizes simulating typical clinical anatomy were created by 2 experienced neurotologists via a standard middle fossa approach, using a diamond burr under an operating microscope. The heads were then immersed in water, the middle cranial fossa defect irrigated to remove trapped air, the bone flap replaced, and soft tissue closed. Of the 2 sets of heads, the first set (6 heads) encompassed the full range of expected dehiscence sizes (from no dehiscence to large dehiscence). The second set (5 heads) focused on small defects and thin bone, based on a subset group of interest observed on data analysis of the first set. Dehiscences created in the second set of heads were measured under the operating microscope (Opmi-1; Zeiss, Oberkochen, West Germany) with a digital micrometer (CD-6''CS, Mitutoyo, Japan).

Each entire head underwent clinical computed tomographic imaging on a Siemens Somatom Sensation 64 scanner (Siemens Medical Solutions, Forchheim, Germany). Helical computed tomographic scanning was done with 0.6-mm collimation, 0.9 pitch, 120 kV, 500 mA. Images were reconstructed with an U80u resolution kernel, into 100 × 100 μm in-plane resolution and 300-μm slice thickness, per our institution's standard superior canal dehiscence scanning protocol. Images were reconstructed in planes parallel to the superior semicircular canal (Pöschl's view) and perpendicular to the canal (Stenver's view). Each temporal bone was then removed with a sagittal saw and otologic drill and trimmed to approximately 120 × 36 mm (a size appropriate for use in the microCT scanner). MicroCT imaging was performed with a Scanco microCT 40 (Scanco Medical AG, Basserdorf, Switzerland), with 70 kVp tube potential, 111 mA tube current, 200 ms interrogation time, and a point-spread function of 0.018 mm. The reconstructed volume of images consisted of 18-μm isotropic voxels.

Clinical CT digital imaging and communications in medicine (DICOM) images were reviewed by 2 experienced, fellowship-trained neuroradiologists (J. S. S. and K. D. V.) using DICOM Works 1.3.5 (Inviweb, France). These neuroradiologists were blinded to the comparison of microCT finding and to the other examiner's observation. DICOM images were windowed by each neuroradiologist to their ''typical'' bone windowing. If the superior semicircular canal (SSC) was read as dehiscent, the image was magnified 200%, and the size of the dehiscence was measured as a line between its bony limits, as described elsewhere (9–11). The lengths of the dehiscences detected on clinical computed tomographic scan were measured in the plane parallel to the canals. Canals in which the parallel view was equivocal for the presence of bone and the perpendicular view showed a dehiscence were excluded from the size-measurement analysis, as neither neuroradiologist felt able to make an accurate assessment of the edges of the dehiscence. Both the parallel (Pöschl's view) and perpendicular (Stenver's view) images were used to make a diagnosis of dehiscent versus intact canal.

The microCT images were then registered to the clinical CT images (one volume mapped onto the other, providing imaging data of 2 scans on the same coordinates) using Analyze software (Analyze Direct, Overland Park, KS, USA). This method has been shown to be reliable in other studies (12–14), and accuracy of registration was verified visually. MicroCT images were 18 μm thick, and the clinical computed tomographic scans were 100 μm thick. The microCT image stacks were then reconstructed into 3-dimensional (3-D) volumes using AMIRA 5.3.3 (Visage Imaging, San Diego, CA, USA). MicroCT measurements were made by 2 examiners who were blinded to the clinical CT findings and the other examiner's results. Two types of measurements were made on microCT: 1) the length of the longest dehiscence present in the entire stack of microCT slices (''2-dimensional [2-D] maximal length''); and 2) the longest dehiscence length on the surface of the 3-D reconstruction of the microCT image volume (''3-D maximal length'').

Statistical analysis and graphical presentation of data was done in Microsoft Excel 2007 and GraphPad Prism (GraphPad Software, La Jolla, CA, USA). Interobserver correlation for the categorical, qualitative analysis of presence or absence of a dehiscence was measured by kappa analysis. For the quantitative measurement of dehiscence length, interobserver reliability was evaluated with Spearman rank-order correlation coefficients. Measurement of dehiscence lengths was evaluated with 2-tailed paired Student's *t* test.

RESULTS

Existence of a Dehiscence

Of the 22 ears, 2 were discarded because of a small air bubble at the location of the dehiscence. Table 1 shows the range of dehiscence sizes and blue lining, detailed for each of the remaining 20 ears. Both neuroradiologists evaluating the clinical CT images found a dehiscence in 19 ears and an intact canal in one. There was 100% concordance between the neuroradiologists for the diagnosis of dehiscent canal versus intact, yielding a kappa statistic of 1.0. MicroCT showed 12 ears to have a dehiscence and 8 to be intact. Figure 1 summarizes these results. Of the 8 canals intact on microCT, 7 seemed erroneously dehiscent on clinical CT, on single view (parallel or perpendicular) or on both views. In 3 of these ears, both the parallel and perpendicular views were read as dehiscent. In the remaining 4 ears, the parallel view was equivocal, but the perpendicular view was read as dehiscent, lending to an overall diagnosis of dehiscence.

TABLE 1. *Specimens included in data analysis*

Case no.	Dehiscence size (cm)
1	3.3
2	3.1
3	4.4
4	3.9
5	Blue-lined
6	Blue-lined
7	1.8
8	Blue-lined
9	4
10	Blue-lined
11	1.1
12	Blue-lined
13	0.6
14	Blue-lined
15	0.4
16	Blue-lined
17	1.1
18	1.8
19	1.1
20	Blue-lined

Clinical CT	MicroCT: Intact	MicroCT: Dehiscent
Intact	1	0
Dehiscent	parallel only: 0 perpendicular only: 4 both views: 3	0 1 11

FIG. 1. Summary of qualitative results.

In 1 ear, the clinical CT parallel view showed an intact canal; however, the perpendicular view showed a dehiscence (overall diagnosis dehiscent), and a very tiny dehiscence existed on microCT. The sensitivity for the diagnosis of dehiscence on clinical CT, compared with gold standard microCT, is 100%, and the specificity is 12.5%.

Figure 2 shows examples of ''false-positives,'' in which clinical CT showed dehiscences, whereas the canals were actually intact on microCT. Figure 2A is a parallel view single-slice clinical CT image, showing a superior canal that was diagnosed as dehiscent by both neuroradiologists. Figure 2B is the registered section of microCT from the same specimen, illustrating intact bone in the location of the presumed dehiscence. Figure 2C is a perpendicular view of a superior canal showing a defect at the canal apex, whereas its corresponding microCT slice in panel D shows intact bone at this location.

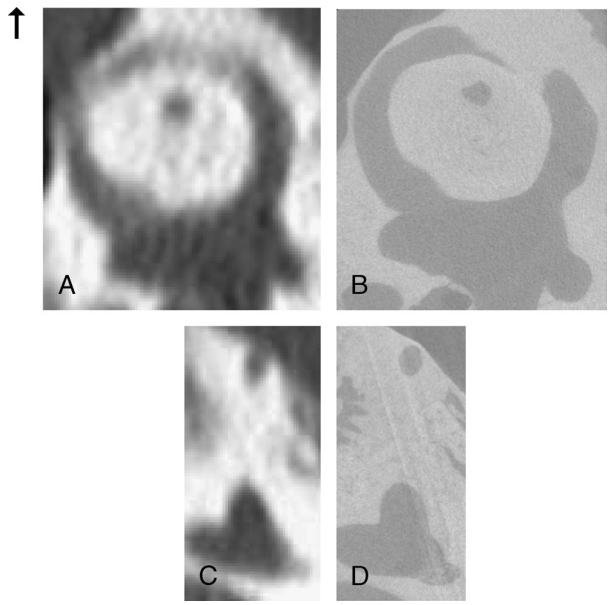

FIG. 2. Example of ''false-positive'' superior canal dehiscence. *A*, Clinical CT oriented parallel to the plane of the semicircular canal (Pöschl's view), read as dehiscent. *B*, MicroCT image of the same ear, displaying intact bone overlying the canal. *C*, Clinical CT image reformatted orthogonal to the superior canal (Stenver's view), also diagnosed as dehiscent. *D*, Corresponding microCT slice, showing intact bone overlying the canal.

Size of a Dehiscence

Dehiscence lengths on clinical computed tomographic scans were measured in the plane parallel to the canal in 14 ears. Length measurements between the 2 neuroradiologists were well correlated (Spearman rank-order correlation coefficient, $r_s = 0.97$; 2-tailed t test, $p < 0.000001$). The average size of dehiscence measured on clinical CT was 3.0 mm (range, 1.6–5.4 mm; standard deviation [SD], 1.3), consistent with sizes observed on clinical CT reported by others (9–11,15).

We used 2 methods to measure the true length of the dehiscence on microCT images. In the first, we measured the ''2-D maximal length'': the longest length dehiscence in the parallel microCT stack, which was registered to the parallel clinical CT stack, and thus in the same *x*-*y*-*z* orientation. In the second method, we measured the longest length of dehiscence on 3-D surface reconstructions of the microCT image volumes (3-D maximal length). Interobserver reliability was excellent (Spearman rank-order correlation coefficient, $r_s = 0.95$ for ''2-D maximal length,'' and $r_s = 0.95$ for ''3-D maximal length,'' 2-tailed, $p = 0.00001$ and $p = 0.000006$, respectively). There was no statistically significant difference between the 2 methods (2-tailed paired t test, $p = 0.12$). To verify that the microCT 3-D surface measurement method produced accurate measurements of dehiscence length, we compared the 3-D maximal lengths with direct measurements using a micrometer of surgically created defects. We found that these lengths were not significantly different (2-tailed paired t test, $p = 0.08$).

Figure 3 shows the dehiscence sizes measured on clinical CT plotted against the sizes measured on microCT. Panel 3A shows this relationship using the 2-D maximal dehiscence length (the longest dehiscence measured on

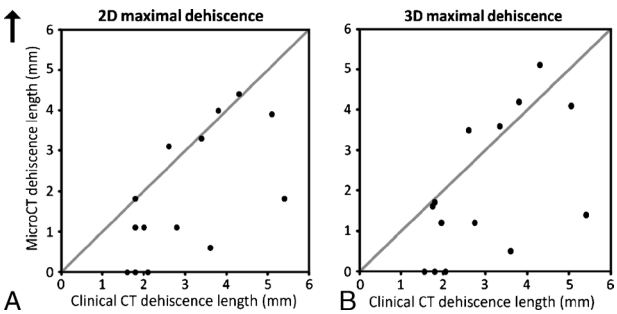

FIG. 3. Dehiscence size measured by microCT and clinical CT. Scatterplot of clinical CT dehiscence lengths (averaged measurement between 2 neuroradiologists) graphed against microCT dehiscence lengths (averaged between 2 observers). *A*, MicroCT data determined by the longest length dehiscence (2-D maximal dehiscence) in the entire stack of microCT images, oriented in same parallel plane as clinical CT. *B*, MicroCT data determined by the longest dimension dehiscence measured on a 3-D surface reconstruction of the microCT image volume (3-D maximal dehiscence). The *gray line* overlying the data represents a perfect correlation between clinical and microCT measurements.

any of the microCT slices, viewed in the same parallel orientation as the corresponding clinical CT). Panel 3B shows this relationship with the 3-D maximal dehiscence length (the longest dimension of dehiscence measured on the 3-D surface reconstruction). The unit slope represents a perfect correlation between lengths measured on clinical and microCT. Points falling below this line are cases in which clinical CT measurements exceed those on microCT. This overestimation of size occurred more frequently in smaller dehiscences. In 3 ears, clinical CT showed dehiscent bone that was actually intact on microCT. Differences between clinical and microCT were statistically significant for both the 2-D maximal length (2-tailed paired t test, $p = 0.004$) and the 3-D maximal length (2-tailed paired t test, $p = 0.02$).

DISCUSSION

High-resolution temporal bone CT is an integral component of the diagnosis and surgical treatment of SSCD syndrome. The data presented here reveal the potential inaccuracy of CT in characterizing small dehiscences and the chance of erroneously identifying a dehiscence in thin, but intact, bone. These findings demonstrate the risk of inaccurate CT diagnosis of canal dehiscence in patients with small defects in clinical CT, leading to the possibility of inappropriate surgical treatment.

Radiologic Issues

We found that microCT was a very good estimate of ''true'' canal length measured directly but was quite different than clinical imaging. This is consistent with a trend of improved diagnosis of superior canal dehiscence with advancing clinical CT technology. Alterations in image reconstruction and finer collimation size have improved diagnostic accuracy for SSCD. For example, 9% to 12% of ears in large study populations showed a superior canal dehiscence on coronal temporal bone CT acquired at 1-mm collimation (16,17). Refining the collimation size from 1 to 0.5 mm led to estimates of the prevalence of 3% in 1 group of 164 ears (18) and 10% in another group of 581 ears (6). Further refinement of the diagnosis arose from reformation of the images into planes parallel and perpendicular to the SSC, reducing the radiologic prevalence of dehiscence to approximately 4% (6,8).

A prevalence of 4% is still greater than the expected 0.5% determined from a large series of cadaveric temporal bones unselected for SSCD, and it is therefore likely to be an overestimate of the true prevalence of SSCD (5). A minor fraction of this difference may be explained by the bias of the radiologic studies toward a population with auditory or vestibular complaints, potentially caused by underlying dehiscence. However, this is likely minimal, as most reports included patients with a wide variety of indications for CT, including trauma, otorrhea, pain, cholesteatoma, and nonspecific auditory and/or vestibular symptoms. In addition, some studies show that few patients with incidental dehiscence on CT fit clinical criteria for superior canal dehiscence syndrome on retrospective analysis (6,17).

Overestimation of SSCD on clinical CT is likely to be due to the partial volume averaging effect (3,6,7). The smallest 3-D volume, or voxel, in a scan is assigned a particular Hounsfield unit based on its radiodensity. If a very thin roof of SSC occupies a minority of a voxel otherwise filled with fluid and soft tissue, its radiodensity is averaged, and the overall radiodensity of the voxel does not suggest the presence of bone. The anatomy of the SSC makes it particularly vulnerable to this effect. Carey et al. (5) observed that 1.4% of temporal bone histologic specimens had bone overlying the superior canal measuring 0.1 mm or thinner. Voxels incorporating this thin, but intact, bone would volume average its density, causing it to falsely appear dehiscent. Finer-cut CTs have improved accuracy, supporting this concept. MicroCT overcomes this problem by providing very small voxels (in this case, 18 μm isotropic), so volume averaging can occur only over a very limited distance. MicroCT was felt to be advantageous over micrometer measurements, as it offered finer resolution and the ability to orient image volumes in the same coordinate system as the clinical CT, allowing direct comparison of measurements made in the same plane. Micrometer measurements were susceptible to being made oblique to the plane of the canal (yielding a different plane than that visualized on clinical CT) and had a fair amount of uncertainty. In addition, microCT permitted careful examination of the intact bone in blue-lined canals.

The data here indicate that clinical CT tends to overestimate the size of smaller dehiscences, particularly those below 3 mm. This is likely due to the curved anatomy of the SSC. If the outer surface of a canal is essentially tangent to the floor of the middle cranial fossa, a small dehiscence will be ringed by thin bone forming an acute angle, but a larger dehiscence will be surrounded by thicker bone forming a wider angle. This greater amount of bone prevents volume averaging from surrounding less-dense tissue, decreasing the apparent size of the defect. The shape of the surgically created dehiscences in our study were similar to those occurring naturally observed in Carey's histologic work, suggesting similar underlying mechanisms (5).

Our findings that clinical CT tends to overestimate the size and prevalence of SSCD are consistent with previous studies evaluating CT. In a patient population with a high pretest probability of dehiscence (those with the typical clinical presentation), the positive predictive value of CT approaches 99% (3). In the general population of patients receiving temporal bone CTs, including those with more vague vestibular symptoms, positive predictive value falls to 57% (6). Together, our data and these previously published data indicate that CT cannot be regarded as a gold standard test and that clinical symptoms must be carefully weighed before a diagnosis is established and surgery recommended. At a high-volume tertiary referral center, the frequency of presentation of

SSCD syndrome may be higher, and CT resolution may be finer, resulting in a more accurate radiologic diagnosis of SSCD on computed tomographic scan. However, because of the low prevalence of SSCD in the general population, the positive predictive value of CT is relatively low. Practitioners may infrequently encounter SSCD syndrome, increasing the risk of misdiagnosis by relying primarily or exclusively on positive CT results. Patients can present with variable symptoms, may have vague complaints, or present with symptoms that overlap with other disorders (4). Otosclerosis, Ménière's disease, perilymphatic fistula, vestibular migraine, and patulous Eustachian tube have features similar to SSCD syndrome (4).

We found that clinical CT images reformatted perpendicular to the plane of the SCC more frequently showed a falsely dehiscent canal than the parallel reformation. It has been shown that coronal sections have a low relative specificity for diagnosis of dehiscence (6,16,17). Although perpendicular slices are cross sections at 90 degrees through the canal (versus coronal sections, which are 45 degrees to the canal), the effects of partial volume averaging in the both cases may be similar. In the parallel orientation, the superior canal is imaged within approximately two 300-μm thick clinical CT slices. The thin roof is captured longitudinally and is surrounded by thick otic capsule on each side of the CT slice. With partial volume averaging, this may seem as more radiopaque than that on the perpendicular view. On the perpendicular view, the sections before and after the slice also contain thin bone, which may result in a volume-averaged darker (thus dehiscent) appearing voxel.

The data presented here may help explain conflicting findings relating clinical symptoms and dehiscence size. Several studies have examined the relation of the size of SSCD measured on CT to clinical symptoms and signs (9–11). Dehiscences larger than 2.5 mm (on CT) have a stronger association with cochleovestibular symptoms and signs, as well as with lower vestibular evoked myogenic potential (VEMP) thresholds (9). Dehiscences smaller than 2.5 mm were associated with either vestibular or cochlear symptoms, rather than both (9). Low frequency air-bone gaps have been reported to be encountered more frequently with larger dehiscences (11). However, others have not found significant relationship between clinical features and size, making the clinical significance of dehiscence size unclear (16). It may be that the findings in some studies were affected by inclusion of false-positive dehiscences on clinical CT. Improved characterization of dehiscence size on computed tomographic scanning may advance further studies of this relationship, as well as aid in understanding the mechanism of other third mobile window lesions.

Relevance for Clinical Decision Making

Anecdotal cases exist in which a dehiscence is found on CT but not encountered on surgical exploration. The findings here underscore this possibility, particularly when the dehiscence found on clinical CT is small. In patients with negative exploration, the syndrome may arise from very thin bone or from microdehiscences or microfractures of thin bone, allowing pressure to transfer between the labyrinth and the intracranial compartment. This situation has been addressed surgically by widening a dehiscence in the presumed area of the defect, and then plugging it, often with improvement of symptoms.

The presence of symptoms, physical examination signs, and ancillary testing, such as audiogram, VEMPs, and temporal bone CT, contribute to the diagnosis of SSCD. Each of these pieces contributes to the larger puzzle; however, individually, they all have varying sensitivity and specificity for SSCD. For example, in 1 study, vertical-torsional nystagmus (evoked by 110 dB) has a sensitivity of 67% and specificity of 100% (19). In the same group of patients, reduced VEMP threshold has been shown to be 80% sensitive and 80% specific for superior canal dehiscence. This study shows that reports evaluating the diagnostic accuracy of symptoms, signs, and test results in patients with suspected SSCD cannot rely on CT as a gold standard (4,19,20).

Many factors influence the resolution of a CT image, such as collimation size, field of view, plane of reformation, image reconstruction algorithms, and much more. Features also can differ among scanner types. The reconstruction kernel and scanner used in this study may not be easily generalized immediately to all other institutions. However, the scanner used here is state of the art and comparable to the scanners used in the literature.

CONCLUSION

Clinical CT is susceptible to error in detecting thin, but intact, bone overlying the SSC. This study illustrates that clinical CT can falsely depict a dehiscence in the setting of thin bone, as well as overestimate the size of smaller dehiscences. Inaccurate diagnosis based on clinical CT is risky, as it may lead to inappropriate surgical treatment. Imaging is still a key to the diagnosis and for surgical planning but must be interpreted with the entire clinical picture, as imaging alone may be misleading. The present study confirms that medical CT cannot be used as the exclusive gold standard for SSCD and that, particularly for small dehiscences on CT, clinical symptoms must be clearly indicative of a dehiscence before surgical treatment is undertaken.

Acknowledgments: The authors thank Dr. Richard Chole for his participation in creating canal fenestrations, Tim Holden for his assistance in image registration, and Nelson Chang for guidance with imaging software.

REFERENCES

1. Minor LB, Solomon D, Zinreich JS, et al. Sound- and/or pressure-induced vertigo due to bone dehiscence of the superior semicircular canal. *Arch Otolaryngol Head Neck Surg* 1998;124:249–58.
2. Minor LB. Clinical manifestations of superior semicircular canal dehiscence. *Laryngoscope* 2005;115:1717–27.

3. Belden CJ, Weg N, Minor LB, et al. CT evaluation of bone dehiscence of the superior semicircular canal as a cause of sound- and/or pressure-induced vertigo. *Radiology* 2003;226:337–43.
4. Zhou G, Gopen Q, Poe DS. Clinical and diagnostic characterization of canal dehiscence syndrome: a great otologic mimicker. *Otol Neurotol* 2007;28:920–6.
5. Carey JP, Minor LB, Nager GT. Dehiscence or thinning of bone overlying the superior semicircular canal in a temporal bone survey. *Arch Otolaryngol Head Neck Surg* 2000;126:137–47.
6. Cloutier JF, Belair M, Saliba I. Superior semicircular canal dehiscence: positive predictive value of high-resolution CT scanning. *Eur Arch Otorhinolaryngol* 2008;265:1455–60.
7. Curtin HD. Superior semicircular canal dehiscence syndrome and multi-detector row CT. *Radiology* 2003;226:312–4.
8. Crovetto M, Whyte J, Rodriguez OM, et al. Anatomo-radiological study of the superior semicircular canal dehiscence radiological considerations of superior and posterior semicircular canals. *Eur J Radiol* 2010;76:167–72.
9. Pfammatter A, Darrouzet V, Gärtner M, et al. A superior semicircular canal dehiscence syndrome multicenter study: is there an association between size and symptoms? *Otol Neurotol* 2010;31:447–54.
10. Rajan GP, Leaper MR, Goggin L, et al. The effects of superior semicircular canal dehiscence on the labyrinth: does size matter? *Otol Neurotol* 2008;29:972–5.
11. Yuen HW, Boeddinghaus R, Eikelboom RH, et al. The relationship between the air-bone gap and the size of superior semicircular canal dehiscence. *Otolaryngol Head Neck Surg* 2009;141:689–94.
12. Skinner MW, Holden TA, Whiting BR, et al. In vivo estimates of the position of advanced bionics electrode arrays in the human cochlea. *Ann Otol Rhinol Laryngol Supp* 2007;197:2–24.
13. Whiting BR, Holden TA, Brunsden BS, et al. Use of computed tomography scans for cochlear implants. *J Digit Imaging* 2008;21: 323–8.
14. Lane JI, Witte RJ, Driscoll CL, et al. Scalar localization of the electrode array after cochlear implantation: a cadaveric validation study comparing 64-slice multidetector computed tomography with microcomputed tomography. *Otol Neurotol* 2007;28:191–4.
15. Krombach GA, DiMartino E, Schmitz-Rode T, et al. Posterior semicircular canal dehiscence: a morphologic cause of vertigo similar to superior semicircular canal dehiscence. *Eur Radiol* 2003;13:1444–50.
16. Ceylan N, Bayraktaroglu S, Alper H, et al. CT imaging of superior semicircular canal dehiscence: added value of reformatted images. *Acta Otolaryngol* 2010;130:996–1001.
17. Williamson RA, Vrabec JT, Coker NJ, et al. Coronal computed tomography prevalence of superior semicircular canal dehiscence. *Otolaryngol Head Neck Surg* 2003;129:481–9.
18. Masaki Y. The prevalence of superior canal dehiscence syndrome as assessed by temporal bone computed tomography imaging. *Acta Otolaryngol* 2011;131:258–62.
19. Crane BT, Minor LB, Carey JP. Three-dimensional computed tomography of superior canal dehiscence syndrome. *Otol Neurotol* 2008;29:699–705.
20. Roditi RE, Eppsteiner RW, Sauter TB, et al. Cervical vestibular evoked myogenic potentials (cVEMPs) in patients with superior canal dehiscence syndrome (SCDS). *Otolaryngol Head Neck Surg* 2009;141:24–8.